


RESEARCH

Open Access



The soluble epoxide hydrolase inhibitor TPPU improves comorbidity of chronic pain and depression via the AHR and TSPO signaling

Ailin Luo^{1†}, Zifeng Wu^{2†}, Shan Li^{1†}, Cindy B. McReynolds⁴, Di Wang², Hanyu Liu², Chaoli Huang^{2,3}, Teng He², Xinying Zhang², Yuanyuan Wang², Cunming Liu², Bruce D. Hammock^{4*}, Kenji Hashimoto^{5*} and Chun Yang^{2*} 

Abstract

Background Patients suffering from chronic pain often also exhibit depression symptoms. Soluble epoxide hydrolase (sEH) inhibitors can decrease blood levels of inflammatory cytokines. However, whether inhibiting sEH signaling is beneficial for the comorbidity of pain and depression is unknown.

Methods According to a sucrose preference test (SPT), spared nerve injury (SNI) mice were classified into pain with or without an anhedonia phenotype. Then, sEH protein expression and inflammatory cytokines were assessed in selected tissues. Furthermore, we used sEH inhibitor TPPU to determine the role of sEH in chronic pain and depression. Importantly, agonists and antagonists of aryl hydrocarbon receptor (AHR) and translocator protein (TSPO) were used to explore the pathogenesis of sEH signaling.

Results In anhedonia-susceptible mice, the tissue levels of sEH were significantly increased in the medial prefrontal cortex (mPFC), hippocampus, spinal cord, liver, kidney, and gut. Importantly, serum CYP1A1 and inflammatory cytokines, such as interleukin 1 β (IL-1 β) and the tumor necrosis factor α (TNF- α), were increased simultaneously. TPPU improved the scores of mechanical withdrawal threshold (MWT) and SPT, and decreased the levels of serum CYP1A1 and inflammatory cytokines. AHR antagonist relieved the anhedonia behaviors but not the allodynia behaviors in anhedonia-susceptible mice, whereas an AHR agonist abolished the antidepressant-like effect of TPPU. In addition, a TSPO agonist exerted a similar therapeutic effect to that of TPPU, whereas pretreatment with a TSPO antagonist abolished the antidepressant-like and analgesic effects of TPPU.

Conclusions sEH underlies the mechanisms of the comorbidity of chronic pain and depression and that TPPU exerts a beneficial effect on anhedonia behaviors in a pain model via AHR and TSPO signaling.

Keywords Chronic pain, Depression, Soluble epoxide hydrolase, TPPU, Translocator protein, Aryl hydrocarbon receptor

[†]Ailin Luo, Zifeng Wu and Shan Li have contributed equally to this work

*Correspondence:

Bruce D. Hammock

bdrhammock@ucdavis.edu

Kenji Hashimoto

hashimoto@faculty.chiba-u.jp

Chun Yang

chunyang@njmu.edu.cn

¹ Department of Anesthesiology, Tongji Hospital, Tongji Medical College, Huazhong University of Science and Technology, Wuhan 430030, China

² Department of Anesthesiology and Perioperative Medicine, The First Affiliated Hospital of Nanjing Medical University, Nanjing 210029, China

³ State Key Laboratory of Pharmaceutical Biotechnology, Model Animal Research Center, Nanjing University, Nanjing 210061, China

⁴ Department of Entomology and Nematology and UC Davis Comprehensive Cancer Center, University of California, Davis, CA 95616, USA

⁵ Division of Clinical Neuroscience, Chiba University Center for Forensic Mental Health, Chiba 260-8670, Japan



Introduction

Pain is an unpleasant feeling or emotional experience accompanied by actual or potential damage to tissues, organs, and nerves [1]. Chronic pain frequently lasts more than three months, is difficult to cure, and is an intractable clinical issue. Depression is a common mental disease that mainly manifests as low mood, anhedonia, and even cognitive impairment [2]. Interestingly, depression is often found accompanying with chronic pain, and depressive symptoms aggravate pain severity and duration. However, the pathophysiology of the comorbidity of chronic pain and depression remains elusive [3, 4]. In this regard, the full elucidation of the mechanisms underlying the comorbidity of chronic pain and depression and the adoption of effective therapeutic strategies are important.

Inflammation plays an important role in developing both pain and depression [5, 6]. Inflammatory cytokines and chemokines act on nociceptors and transmit the deleterious stimulus to the central nervous system, resulting in abnormal or overactivated neuroinflammation [7, 8]. In addition, inflammatory cytokines also appear in the cortices and hippocampi of brain tissues in patients with major depressive disorder [9]. The hyperactivity and hyperexcitability of neurons characterize central sensitization in the brain and spinal cord, originating from persistent nociceptive input during chronic pain [8]. Therefore, inflammation is likely to play a critical role in the pathogenesis of chronic pain and depression. Resolving the overactivated inflammatory system might benefit the recovery of the comorbidity of pain and depression.

The metabolism of arachidonic acid (ARA) via cytochrome P450s (CYP450s) produces epoxy fatty acids (EpFAs), which provide protective effects in inflammatory disorders [10]. Eicosanoids are metabolites of ARA and other long chain fatty acids. The long fatty acids can be epoxidized by CYP450 to produce four regioisomeric epoxyeicosatrienoic acids (EETs) (i.e., 5,6-EET, 8,9-EET, 11,12-EET, and 14,15-EET). Moreover, omega-3 polyunsaturated fatty acids (PUFAs), such as eicosapentaenoic acid (EPA) and docosahexaenoic acid (DHA), can also be catalyzed into epoxyeicosatetraenoic acids (EEQs) and epoxydocosapentaenoic acids (EDPs), collectively referred to as epoxy-fatty acids (EpFAs) [11]. EETs and other EpFAs can reduce the release of the vascular cell adhesion molecule 1 (VCAM-1), intercellular adhesion molecule 1 (ICAM-1), and endothelial cell-selective adhesion molecule (E-selectin). They can also inhibit the nuclear factor κ B (NF- κ B) signaling pathway, exerting anti-inflammatory and neuroprotective effects [12–14]. Soluble epoxide hydrolase (sEH, encoded by the *Ephx2* gene) catalyzes the hydrolysis of EETs to dihydroxyeicosatrienoic acids (DHETs) with lower biologically activity [15]

and far greater polarity. In the human brain, sEH occurs in neurons, oligodendrocytes, astrocytes, and ependymal cells [16]. Numerous studies have shown that sEH inhibitors (sEHIs) can treat neuropathic pain and inflammatory pain [17, 18]. Importantly, sEH levels in the parietal cortex were higher in patients with major depressive disorders compared with control subjects [19]. sEH improved the behavioral performance of mice with lipopolysaccharide (LPS)-induced depression-like behavior and induced the release of the regulatory neurotrophic factor [20, 21]. Therefore, therapeutic strategies aimed at inhibiting sEH might have the pharmacological benefit of curing chronic pain–depression comorbidity.

sEH helps transform the anti-inflammatory products of CYP epoxidation into inactive diols [22]. CYPs comprise various subfamilies, such as CYP1A, CYP1B, etc. [23]. The aryl hydrocarbon receptor (AHR) is a transcription factor expressed in the cytosol which translocates to the nucleus after binding to its ligands. After dimerization with the AHR nuclear translocator (ARNT), AHR/ARNT dimers bind to the enhancer region of the *CYP1A1* and other genes [24, 25]. In the metabolism of PUFAs, multiple CYPs produce EETs by epoxidation, as well as hydroxylation of ARA and other PUFAs, to pro-inflammatory hydroxyeicosatetraenoic acids (HETEs) [26, 27]. In association with immune/inflammatory diseases, an increased AHR level appears in patients with major depression and multiple sclerosis [28]. Excessive activation of AHR impaired the differentiation and proliferation of hippocampal neural progenitor cells, thus affecting neurogenesis and cognitive function [29]. Collectively, these findings indicate that the sEH–AHR signaling pathway may be involved in pro-inflammatory effects by regulating the metabolism of PUFAs.

In contrast to sEH and AHR, the translocator protein (TSPO) plays an anti-inflammatory role by transporting cholesterol [30]. TSPO is located in the outer mitochondrial membrane and transports cholesterol to the inner membrane, leading to the synthesis of neurosteroids in the CNS [31]. The activation of TSPO ameliorates chronic inflammatory and neuropathic pain [32, 33]. Increased cholesterol levels in the brain are frequently associated with neurodegenerative diseases and neuroinflammation [34]. In turn, the normalization of cholesterol metabolism in spinal microglia reduced the release of inflammatory cytokines and relieved chronic neuropathic pain [35]. Moreover, the TSPO ligand antagonizes the neurotoxic effects mediated by *N*-methyl-D-aspartate receptors, inducing antidepressant and antianxiety effects [36]. Interestingly, EETs exerted a cholesterol-lowering effect, and both *Ephx2* knockout and sEH reduced plasma cholesterol levels [37, 38].

The purpose of the present study was to elucidate the role of sEH in the chronic pain–depression comorbidity induced by SNI surgery. We planned to investigate the effects of the sEH inhibitor TPPU on post-operative symptoms of hyperalgesia and anhedonia and detect changes in TSPO and AHR levels in selected tissues. This study's findings suggest that the alleviation of the pain–depression comorbidity by sEH inhibitors occurs via distinct signaling pathways involving TSPO or AHR. This will provide important tools and approaches for studying mechanisms underlying the similarities and differences of the comorbidity of pain and depression.

Materials and methods

Animals

Two month-old male C57BL/6 mice (body weight 20–25 g) were purchased from the Animal Center of Tongji Hospital in this study. Animals were acclimated to the environmental conditions for 7 days before the experiment. Animals were housed in controlled temperature (22 ± 2 °C.) and 12 h light/dark cycles (lights on 8:00) with food and water ad libitum. The study was conducted in strict accordance with the recommendations in the Guide for the Care and Use of Laboratory Animals and under protocols approved by the Experimental Animal Committee of Tongji Hospital, Tongji Medical College, Huazhong University of Science and Technology (Wuhan, China).

Spared nerve injury

The SNI surgery was performed as previous described [39]. Briefly, the 3 peripheral branches (sural, common peroneal, and tibial nerves) of left sciatic nerve were exposed under general anesthesia of 1.5–2.5% isoflurane. The tibial and common peroneal nerves were ligated with 6-0 silk suture and cut off the distal to the ligation, while nerves were exposed but not transected for sham surgery.

Behavioral tests

All behavioral procedures were conducted in the dark phase (active for mice) of the daily light/dark cycle. To reduce the influence of artificial factors on results, the individual who carried out the tests and data analysis was blind to the experimental assignments, and all animals were tested under consistent conditions and using the same apparatus.

MWT

Before MWT, mice were placed in plexiglass chambers with a wire net floor for 30 min in consecutive 6 days to acclimate to the test conditions. Mechanical allodynia was measured as previously described [40, 41]. The

Von Frey monofilaments were applied to the lateral 1/3 of left paws using the up-and-down method. The paws quick withdrawal or flinching was considered as a positive response. All filament stimuli were applied 4 times with a period of 30 s interval.

SPT

Mice were feed separately and exposed to two identical bottles (tap water and 1% sucrose solution) for 48 h, and the bottles were exchanged every 24 h to avoid place preference. Mice were followed by 24 h of water and food deprivation and 24 h exposure to two identical bottles. The bottles containing water and sucrose were weighed before and at the end of this period and the sucrose preference was determined.

Experiment design

Study 1: SNI on mechanical allodynia, anhedonia-like symptoms and sEH protein expression

To assess the effects of chronic pain on anhedonia and sEH protein expression, 26 mice were randomly divided into two groups (Sham, $n=8$; SNI, $n=18$), baseline threshold of mechanical allodynia was undertaken on 1 day before SNI and re-measured on day 7, 14, 21 after surgery. Sucrose preference test (SPT) was performed on day 5, 12 and 19 after SNI to assess the anhedonia-like symptoms. On day 22 after surgery, clustering analysis according to SPT scores was performed to divide SNI mice into SNI with anhedonia susceptible group (Anhedonia susceptible, $n=8$) and SNI without anhedonia (Anhedonia resilient, $n=10$). Samples were collected on day 23 postoperatively after anesthesia of isoflurane.

Study 2: TPPU alleviated mechanical allodynia and anhedonia-like symptoms associated with TSPO signaling and AHR signaling

To determine the effects of TPPU on mechanical allodynia and anhedonia, 56 mice were randomly assigned two groups (sham, $n=16$; SNI, $n=40$). On day 15, clustering analysis according to SPT scores was performed to divide SNI mice into SNI with anhedonia susceptible group (Anhedonia susceptible; $n=16$) and SNI without anhedonia (Anhedonia resilient; $n=24$). Vehicle (30% PEG 400) or TPPU (3 mg/kg, dissolved in PEG 400), a sEH inhibitor, was administered orally to one of four groups ($n=8$ per group): sham group treated daily with vehicle or TPPU, anhedonia susceptible mice with vehicle or TPPU. MWT was performed 30 min after consecutive 7 days treatment. SPT was undertaken to evaluate the

therapeutic effects of TPPU on anhedonia-like symptoms 21 days after surgery. Samples were collected on day 23 postoperatively after anesthesia of isoflurane.

Study 3: AHR agonist offset the antidepressant but not analgesia effects of TPPU

To determine the role of AHR in the therapeutic effects of TPPU on chronic pain and anhedonia, 66 mice were divided into two groups (Sham, $n=6$; SNI, $n=60$). Similarly, anhedonia susceptible mice selected from SNI group by clustering with SPT scores, and then were randomly assigned to 4 groups: anhedonia susceptible without any compounds (Sus, $n=6$), anhedonia susceptible daily treated with CH-223191 (10 mg/kg, dissolved in corn oil) from day 15 for consecutive 7 days (Sus + CH-223191, $n=6$), anhedonia susceptible treated with FICZ (100 ug/kg, dissolved in corn oil) on day 15 (Sus + FICZ, $n=6$), and anhedonia susceptible simultaneously treated with FICZ and TPPU on day 15, thereafter treated with TPPU solely for consecutive 6 days (Sus + FICZ + TPPU, $n=6$). Behavioral tests were performed as the same as study 3. Samples were collected on day 23 postoperatively after anesthesia of isoflurane.

Study 4: TSPO antagonists offset the antidepressant and analgesia effects of TPPU

To determine the role of TSPO in the therapeutic effects of TPPU on chronic pain and anhedonia, 110 mice were divided into two groups (Sham, $n=8$; SNI, $n=102$). Similarly, anhedonia susceptible mice selected from SNI group by clustering with SPT scores, and then were randomly assigned into 4 groups: anhedonia susceptible without any compounds (Sus, $n=8$), anhedonia susceptible daily treated with TPPU (3 mg/kg, dissolved in PEG 400) from day 15 for consecutive 7 days (Sus + TPPU, $n=8$), anhedonia susceptible treated with Finasteride (10 mg/kg, dissolved in corn oil), TPPU (3 mg/kg) from day 15 for consecutive 7 days (Sus + Fina + TPPU, $n=8$), and anhedonia susceptible simultaneously treated with PK-11195 (3 mg/kg, dissolved in 2% DMSO and 0.8% Tween) and TPPU (3 mg/kg) from day 15 to day 21 (Sus + PK + TPPU, $n=8$), anhedonia susceptible with AC5216 (1 mg/kg, suspended in 0.5% tragacanth gum aqueous solution) from day 15 to day 21 (Sus + AC, $n=8$). Behavioral tests were performed as the same as study 2 or study 3. Samples were collected on day 23 postoperatively after anesthesia of isoflurane.

Drug administration

The SEH inhibitor TPPU was synthesized at Professor Bruce Hammock's lab (University of California, Davis). TPPU (3 mg/kg) was dissolved in 20% (vol/vol)

polyethylene 400 (PEG 400, Cat#P8530, Solarbio, Beijing) [21]. The AHR inhibitor CH-223191 (10 mg/kg, HY-12684, MedChemExpress, USA) and AHR agonist FICZ (100 ug/kg, HY-12451, MedChemExpress, USA) were dissolved in corn oil and intragastrically administered as previously described [42, 43]. TSPO antagonist PK-11195 (3 mg/kg, ab120378, Abcam, UK) was dissolved in 2% DMSO and 0.8% Tween and then diluted by saline. Finasteride (10 mg/kg, HY-13635, MedChemExpress, USA), a 5α -reductase inhibitor, was dissolved in corn oil. The above two reagents were previously reported to block the effects of TSPO overexpression [44]. AC-5216 (1 mg/kg, HY-15527, MedChemExpress, USA) were suspended in 0.5% tragacanth gum aqueous (CAT#G9390, Solarbio, Beijing) solution for oral administration, which was reported to induce antianxiety and antidepressant effects [45].

Western blot analysis

As described previously, tissues were grated and homogenized with RIPA buffer (Boster, Wuhan, China) at 4 °C for 30 min, then centrifuged and supernatants were collected. The protein concentrations in supernatants were determined by BCA protein assay kit (Boster, Wuhan, China). The protein samples were separated by 10% sodium dodecyl sulfate–polyacrylamide gel (SDS-PAGE) electrophoresis, and then were transferred to poly vinylidene fluoride (PVDF) membranes (Millipore, Bedford, MA, USA). Bands were blocked with 5% BSA dissolved in TBST (0.1% Tween 20 in Tris-buffered saline) for 1 h at room temperature. Relative primary antibodies were incubated at 4 °C overnight: rabbit EPHX-2 (1:5000, ab155280, Abcam), rabbit AHR (1:500, AF6278, Affinity), rabbit TSPO (1:1000, DF8227, Affinity), and rabbit GAPDH (1:5000, AF7021, Affinity). After warming and washing by TBST, second antibody was incubated on bands for 2 h at room temperature: goat anti-rabbit IgG horseradish peroxidase (1:5000, Promotor, Wuhan, China). Finally, these protein bands were visualized by enhanced chemiluminescence substrate solutions (Promotor, Wuhan, China) with the ChemiDoc XRS chemiluminescence imaging system (Bio-Rad, Hercules, CA, USA).

ELISA

The IL-6, IL-1 β , TNF- α , CYP1A1 and CYP1B1 ELISA kits were purchased from MDL Biotech (Beijing, China; $n=6$ or 8 for each group). The serum samples were prepared from whole heart blood samples after centrifugation at $3000 \times g$ for 10 min. The 10 μ l samples and 60 μ l dilution buffer were added to the wells followed by incubation at room temperature for 60 min. Then

washing the plates and adding zymolytes into the wells, the absorbance was measured on a spectrophotometer at 450 nm. The concentrations were calculated to the amount of standard protein of each sample.

AHR CALUX cell bioassay [46]

Chemicals

TPPU was dissolved in DMSO and provided by EICOSIS at a concentration of 10 mM for use in CALUX bioassay analysis of their agonist and antagonist activity at 10 μ M final incubation concentration.

Bioassay analysis

Recombinant mammalian cells were incubated at the indicated concentration for 24 h, in the absence of reference standard (for agonist activity) or presence of reference standard (antagonist activity), the cells lysed and luciferase activity determined in a microplate luminometer following automatic injection of the reagent (luciferin). The luciferase activity of cells incubated with sample extracts was directly compared to that of cells incubated with negative and positive control chemicals relevant for each bioassay, results expressed as a percent of the maximal induced activity of the respective positive control chemical (after subtraction of background activity) and positive samples confirmed by statistical analysis.

The specific cell bioassays that were run on these two sets of samples included:

1. Human Ah receptor (AHR)-responsive liver cancer cell bioassay for AHR active chemicals (HG2L6.1c1 cells).
2. Mammalian cell lines to detect cytotoxicity (all of the above lines were used for this).

Cytotoxicity assessment

Cell viability/cytotoxicity was assessed for all experiments using nuclear receptor cell lines using a scaled qualitative visual observation method previously approved by OECD (2016) and ICCVAM (2011) for the VM7Luc4E2 cells that scores viability on a scale of 1 (normal) to 4 (significant loss of viability). Cytotoxicity by this method is identified if cells exhibit any change in normal cell morphology or cell density (the latter resulting from cell death and/or cells detaching from the culture plate). Since no cytotoxicity was observed in any cell line with any chemical or extract treatment they were assigned a score of 1 (Normal

Cell Morphology and Cell Density (for details see Table 11–1 in ICCVAM, 2011)).

Statistical analysis

The data are shown as the mean \pm standard error of the mean (SEM). Analysis was performed using GraphPad prism software version 7.0. Leven's test and Shapiro–Wilk's test were used to analyze the homoscedasticity and normality of each dataset. Comparisons among groups were performed using the one-way analysis of variance (ANOVA) or two-way ANOVA, followed by post hoc Tukey test. For different time-points, two-way repeated ANOVA were performed to compare the difference among groups. If the dataset did not follow a normal distribution or homoscedasticity, non-parametric analyses were introduced to the dataset via Kruskal–Wallis and Mann–Whitney two-sided statistical analyses. In hierarchical cluster analysis, the data were firstly standardized by z scores. Then, hierarchical cluster analysis of SPT was performed using Ward's method and applying squared Euclidean distance as the distance measure, and mice were classified as anhedonia susceptible or resilient [47]. The P-values of less than 0.05 were considered statistically significant.

Results

Altered expression of the sEH protein in selected tissues in sham, anhedonia-susceptible, and anhedonia-resilient mice

A total of 18 mice with SNI were classified into anhedonia-susceptible and anhedonia-resilient groups via a hierarchical analysis according to SPT scores (Fig. 1B and Additional file 1: Table S1). The MWT of both anhedonia-susceptible and -resilient mice was dramatically lower than that of the sham group on days 7, 14, and 21 after surgery (Fig. 1C). The SPT scores in anhedonia-susceptible mice were decreased on days 5, 12, and 19 after SNI (Fig. 1D). There were significant changes in the level of sEH in the mPFC, hippocampus, spinal cord, liver, kidney, and gut, but not in the ACC, NAc, striatum, cerebellum, heart, muscle, and blood vessels in anhedonia-susceptible and -resilient mice compared with sham mice (Fig. 2A). These findings suggest that the levels of the sEH protein in selected brain regions might confer susceptibility to chronic neuropathic pain. Next, we investigated the correlations between sEH levels and MWT in selected tissues. Significant negative correlations occurred in tissues such as the mPFC, hippocampus, spinal cord, liver, kidney, and gut (Fig. 2B–G). Furthermore, there was a positive correlation between MWT and SPT scores (Fig. 2H).

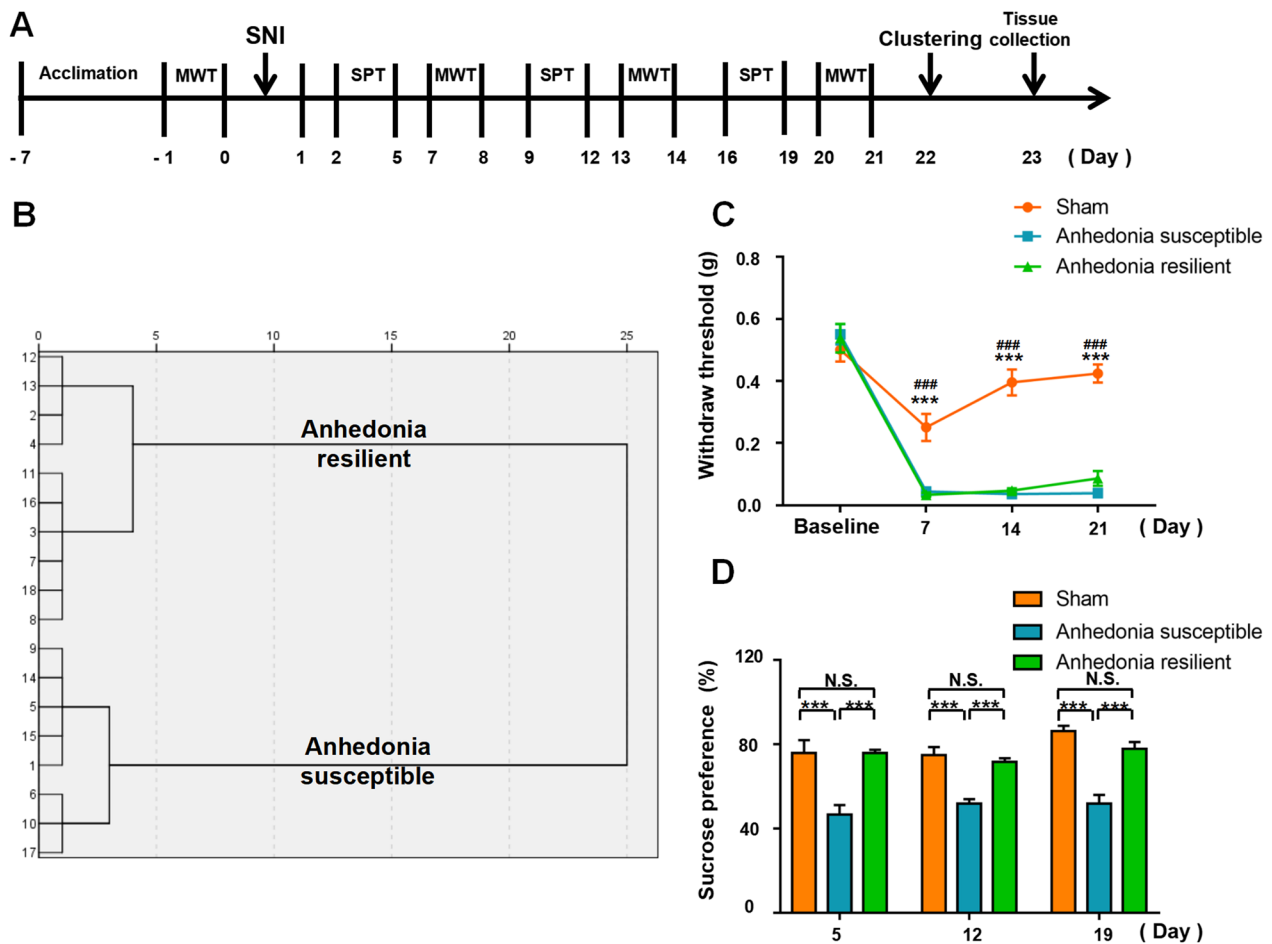


Fig. 1 Behavioral results in sham, anhedonia-susceptible, and anhedonia-resilient mice. **A** Schedule of the experiment. SNI surgery was performed after acclimation. MWT was measured on days 7, 14, and 21 after SNI. The SPT was performed on days 5, 12, and 19 after SNI. **B** Dendrogram of the hierarchical clustering analysis. A total of 18 SNI mice were classified into anhedonia-susceptible and anhedonia-resilient groups by a hierarchical cluster analysis of the SPT results. **C** MWT [Time: $F(3, 21) = 124.2, P < 0.001$; Group: $F(2, 14) = 118, P < 0.001$; Interaction: $F(6, 42) = 17.12, P < 0.001$] was measured on days 7, 14, and 21 in the sham, anhedonia-resilient, and anhedonia-susceptible groups after SNI. $***P < 0.001$, susceptible group vs. sham group; $###P < 0.001$, resilient group vs. sham group. **D** SPT [Time: $F(2, 14) = 1.873, P = 0.19$; Group: $F(2, 14) = 49.95, P < 0.001$; Interaction: $F(4, 28) = 1.616, P = 0.20$] was measured in the sham, anhedonia-resilient, and anhedonia-susceptible groups on days 5, 12, and 19 after SNI. $***P < 0.001$. MWT mechanical withdrawal threshold, SNI spared nerve injury, SPT sucrose preference test

Alleviation of mechanical allodynia and anhedonia-like symptoms in anhedonia-susceptible mice after TPPU treatment

Sixteen anhedonia-susceptible mice were selected after hierarchical cluster analysis of SPT scores (Fig. 3A, 3B and Additional file 1: Table S2). To detect the effects of TPPU on mechanical allodynia and anhedonia, we treated the sham group and anhedonia-susceptible mice daily with vehicle or TPPU (3 mg/kg) for 7 consecutive days. TPPU improved the decreased SPT scores and increased the decreased scores of MWT in anhedonia-susceptible mice (Fig. 3C, D). After administration of

TPPU, the levels of sEH were decreased significantly in the hippocampus, spinal cord, liver, kidney, and gut, but not in the mPFC of anhedonia-susceptible mice compared to the sham group (Fig. 3I). Intriguingly, two contradictory trends emerged regarding TSPO and AHR signaling. The AHR levels were increased in the hippocampus, liver, kidney, and gut but not in the mPFC and spinal cord of anhedonia-susceptible mice. In contrast, the TSPO levels were decreased in the hippocampus, spinal cord, and kidney in the anhedonia-susceptible group. Finally, TPPU reversed these changes (Fig. 3J–K). Our results indicated a similar

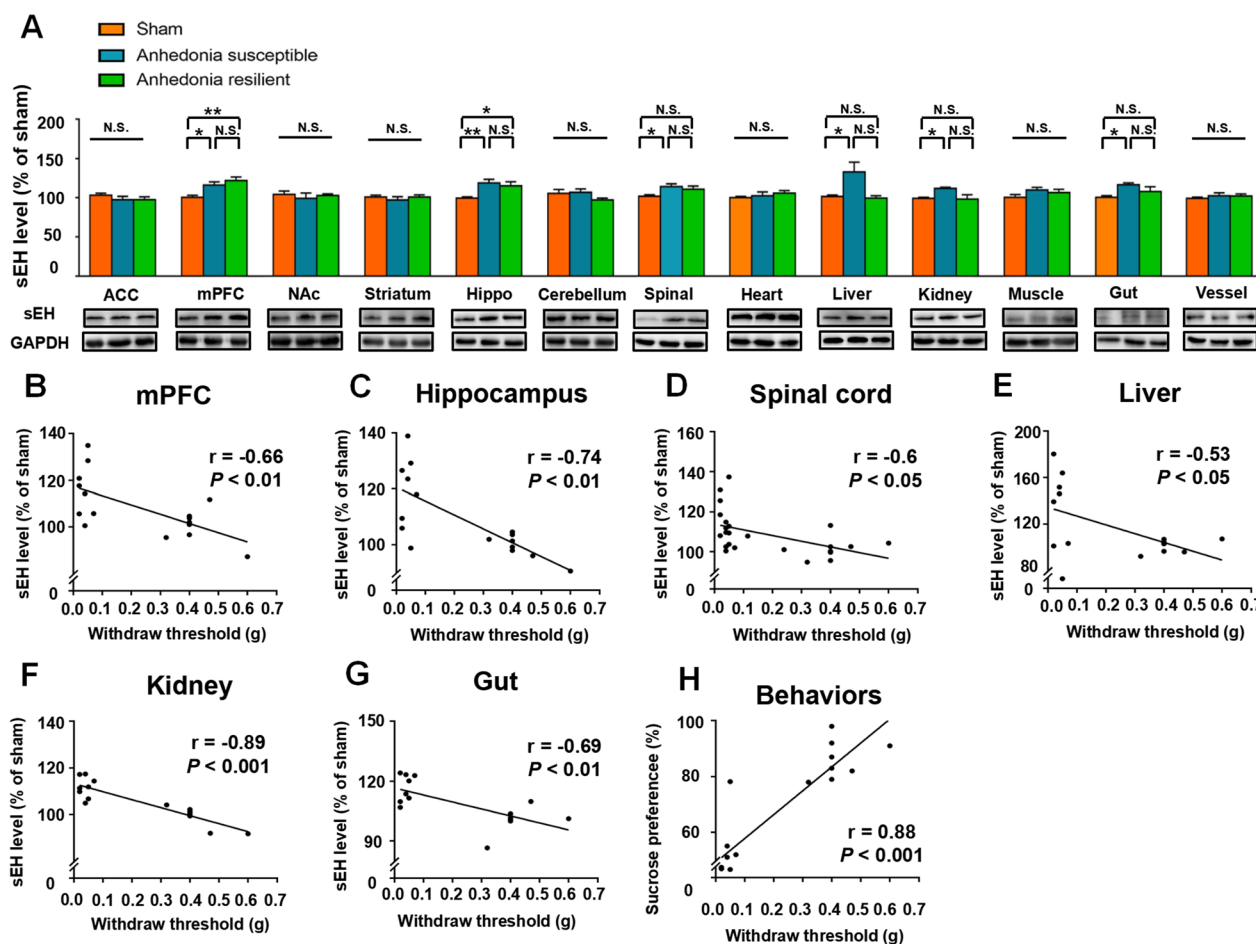


Fig. 2 sEH levels in selected tissues from sham, anhedonia-susceptible, and anhedonia-resilient mice. **A** Levels of the sEH protein in selected tissues. ACC [$H_2 = 1.865$, $P = 0.394$]; mPFC [$F(2, 21) = 8.615$, $P < 0.01$]; NAc [$H_2 = 0.620$, $P = 0.733$]; Striatum [$H_2 = 0.695$, $P = 0.706$]; Hippo [$F(2, 21) = 6.145$, $P < 0.01$]; Cerebellum [$F(2, 21) = 2.75$, $P = 0.087$]; Spinal cord [$F(2, 21) = 3.457$, $P = 0.05$]; Heart [$H_2 = 2.945$, $P = 0.229$]; Liver [$F(2, 21) = 6.214$, $P < 0.01$]; Kidney [$F(2, 21) = 4.945$, $P < 0.05$]; Muscle [$F(2, 21) = 1.554$, $P = 0.235$]; Gut [$H_2 = 7.338$, $P < 0.05$]; Vessels [$F(2, 21) = 0.4566$, $P = 0.64$]. * $P < 0.05$; ** $P < 0.01$; *** $P < 0.001$. **B** Correlations between sEH levels and MWT scores in the mPFC ($R^2 = 0.4302$, $P < 0.01$); **C** correlations between sEH levels and MWT scores in the hippocampus ($R^2 = 0.547$, $P < 0.01$); **D** correlations between sEH levels and MWT scores in the spinal cord ($R^2 = 0.3576$, $P < 0.05$); **E** correlations between sEH levels and MWT scores in the liver ($R^2 = 0.2829$, $P < 0.05$); **F** correlations between sEH levels and MWT scores in the kidney ($R^2 = 0.8007$, $P < 0.001$); **G** correlations between sEH levels and MWT scores in the gut ($R^2 = 0.476$, $P < 0.01$); **H** correlations between MWT and SPT scores ($R^2 = 0.7731$, $P < 0.001$). ACC anterior cingulate cortex, mPFC medial prefrontal cortex, MWT mechanical withdrawal threshold, NAc nucleus accumbens, NS not significant, SNI spared nerve injury, SPT sucrose preference test

tendency between the levels of sEH and AHR, but an opposite trend between the levels of sEH and TSPO. In addition, we examined the levels of inflammatory cytokines and showed that the serum concentrations of CYP1A1, IL-1 β , and TNF- α were increased in anhedonia-susceptible mice. In contrast, a decrease in the serum levels of CYP1A1, IL-1 β , and TNF- α occurred after TPPU treatment (Fig. 3E–H). These data suggest that TPPU exerts its beneficial effects via the inhibition of AHR signaling and the activation of TSPO signaling.

An AHR agonist attenuated the antidepressant-like effects of TPPU

Mice with SNI-induced anhedonia were selected by hierarchical cluster analysis of SPT scores (Fig. 4A, B, Additional file 1: Fig. S1, and Additional file 1: Tables S3 and S4). We administered an AHR agonist (FICZ, 100 μ g/kg), an AHR antagonist (CH-223191, 10 mg/kg), and TPPU (3 mg/kg) to anhedonia-susceptible mice. Pain relief behaviors occurred after treating anhedonia-susceptible

mice with TPPU and FICZ (Fig. 3C). More importantly, CH-223191 alone restored the decreased SPT scores in anhedonia-susceptible mice (Fig. 3D). CH-223191 exerted pharmacological benefits regarding inhibited levels of CYP1A1, IL-1 β , and TNF- α , but not of CYP1B1. The serum IL-1 β level was decreased after the combined utilization of TPPU and FICZ in anhedonia-susceptible mice (Fig. 3E–H). In the hippocampus and gut, the levels of the sEH protein were decreased in anhedonia-susceptible mice that received FICZ and TPPU (Fig. 3I). In addition, CH-223191 decreased the sEH level in the hippocampus, liver, kidney, and gut. Moreover, the combined use of FICZ and TPPU also decreased the AHR levels in anhedonia-susceptible mice (Fig. 3J). In addition, we also found TPPU is neither an agonist nor an antagonist in the AHR CALUX cell bioassay and that no cytotoxicity was observed at a concentration of 10 μ M in the incubation (Table. 1).

Conversely, the levels of the TSPO protein were increased in the hippocampus and spinal cord in

anhedonia-susceptible mice after the administration of FICZ and TPPU (Fig. 3K). These results indicate that the AHR antagonist exert the antidepressant-like effect similar to TPPU, whereas no change in its analgesic effect appeared in anhedonia-susceptible mice. These findings suggest that the downregulation of AHR may improve the SPT scores in anhedonia-susceptible mice.

Both the antidepressant-like and analgesic effects of TPPU were attenuated after treatment with a TSPO antagonist

Anhedonia-susceptible mice were selected and treated with a TSPO agonist (AC5216), TSPO antagonists (PK-11195 and Finasteride), and TPPU (Fig. 5A, B, Additional file 1: Fig. S2, and Additional file 1: Tables S5 and S6). AC5216 exerted antidepressant-like and analgesic effects similar to those of TPPU in anhedonia-susceptible mice (Fig. 5C and D). Furthermore, TPPU reduced serum CYP1A1 in anhedonia-susceptible mice (Fig. 5E–H). Therefore, the activation of TSPO signaling by TPPU may have effective antidepressant-like and analgesic effects in anhedonia-susceptible mice.

(See figure on next page.)

Fig. 3 Effects of TPPU on MWT and SPT scores and on the levels of sEH, AHR, and TSPO. **A** Schedule of the experiment. SNI surgery was performed after acclimation. TPPU (3 mg/kg, once daily) was administered orally for 7 consecutive days, starting at day 14 after SNI. MWT was measured on days 7, 14, 15, 16, 17, 18, 19, 20, and 21 after SNI. The SPT was performed on days 5, 12, and 21 after SNI. **B** Dendrogram of the hierarchical clustering analysis. A total of 40 SNI mice were classified into anhedonia-susceptible and anhedonia-resilient groups via a hierarchical cluster analysis of the SPT results. **C** MWT [Time: $F(9, 63) = 19.33, P < 0.001$; Group: $F(3, 21) = 173.5, P < 0.001$; Interaction: $F(27, 189) = 7.369, P < 0.001$] was measured on days 7, 14, 15, 16, 17, 18, 19, 20 and 21 in the Sham + Veh, Sham + TPPU, Sus + Veh, and Sus + TPPU groups after SNI. $^{***}P < 0.001$, Sham + Veh group vs. Sus + Veh group; $^{###}P < 0.001$, Sus + Veh group vs. Sus + TPPU group. **D** SPT [Time: $F(1, 56) = 10.34, P < 0.01$; Group: $F(3, 56) = 33.17, P < 0.001$; Interaction: $F(3, 56) = 8.744, P < 0.001$] was performed in the Sham + Veh, Sham + TPPU, Sus + Veh, and Sus + TPPU groups on days 12 and 21 after SNI. $^{**}P < 0.01$, $^{***}P < 0.001$. **E** CYP1A1 level in the serum [TPPU: $F(1, 20) = 10.73, P < 0.01$; Group: $F(1, 20) = 8.407, P < 0.01$; Interaction: $F(1, 20) = 22.69, P < 0.001$]. **F** CYP1B1 level in the serum [TPPU: $F(1, 20) = 1.241, P = 0.28$; Group: $F(1, 20) = 0.06, P = 0.8$; Interaction: $F(1, 20) = 0.436, P = 0.52$]. **G** IL-1 β level in the serum [TPPU: $F(1, 20) = 8.976, P < 0.01$; Group: $F(1, 20) = 4.557, P < 0.05$; Interaction: $F(1, 20) = 11.16, P < 0.01$]. **(H)** TNF- α level in the serum [TPPU: $F(1, 20) = 55.45, P < 0.001$; Group: $F(1, 20) = 88.65, P < 0.001$; Interaction: $F(1, 20) = 55.45, P < 0.001$]. **I** Effects of TPPU on sEH expression. mPFC [TPPU: $F(1, 28) = 0.1376, P = 0.71$; Group: $F(1, 28) = 1.615, P = 0.21$; Interaction: $F(1, 28) = 0.2046, P = 0.65$]; hippocampus [TPPU: $F(1, 28) = 18.62, P < 0.001$; Group: $F(1, 28) = 3.055, P = 0.09$; Interaction: $F(1, 28) = 15.77, P < 0.001$]; spinal cord [TPPU: $F(1, 28) = 11.33, P < 0.001$; Group: $F(1, 28) = 0.1966, P = 0.67$; Interaction: $F(1, 28) = 15.28, P < 0.001$]; liver [TPPU: $F(1, 28) = 44.43, P < 0.001$; Group: $F(1, 28) = 2.362, P = 0.14$; Interaction: $F(1, 28) = 10.38, P < 0.01$]; kidney [TPPU: $F(1, 28) = 51.25, P < 0.001$; Group: $F(1, 28) = 1.287, P = 0.26$; Interaction: $F(1, 28) = 9.837, P < 0.01$]; gut [TPPU: $F(1, 28) = 18.49, P < 0.001$; Group: $F(1, 28) = 3.879, P = 0.06$; Interaction: $F(1, 28) = 15.33, P < 0.001$]. $^{*}P < 0.05$, $^{**}P < 0.01$, $^{***}P < 0.001$. **J** Effects of TPPU on AHR expression. mPFC [TPPU: $F(1, 28) = 0.0119, P = 0.91$; Group: $F(1, 28) = 0.016, P = 0.9$; Interaction: $F(1, 28) = 0.1949, P = 0.66$]; hippocampus [TPPU: $F(1, 28) = 18.04, P < 0.001$; Group: $F(1, 28) = 1.015, P = 0.32$; Interaction: $F(1, 28) = 10.42, P < 0.01$]; spinal cord [TPPU: $F(1, 28) = 0.6641, P = 0.42$; Group: $F(1, 28) = 1.8, P = 0.19$; Interaction: $F(1, 28) = 2.695, P = 0.11$]; liver [TPPU: $F(1, 28) = 10.73, P < 0.01$; Group: $F(1, 28) = 44.97, P < 0.001$; Interaction: $F(1, 28) = 8.917, P < 0.01$]; kidney [TPPU: $F(1, 28) = 39.57, P < 0.001$; Group: $F(1, 28) = 5.957, P < 0.05$; Interaction: $F(1, 28) = 21.38, P < 0.001$]; gut [TPPU: $F(1, 28) = 5.764, P < 0.05$; Group: $F(1, 28) = 59.08, P < 0.001$; Interaction: $F(1, 28) = 6.479, P < 0.05$]. Data are reported as the mean \pm SEM ($n = 8$). $^{*}P < 0.05$, $^{**}P < 0.01$, $^{***}P < 0.001$. **K** Effects of TPPU on TSPO expression. mPFC [TPPU: $F(1, 28) = 0.0844, P = 0.77$; Group: $F(1, 28) = 0.0057, P = 0.94$; Interaction: $F(1, 28) = 0.4106, P = 0.53$]; hippocampus [TPPU: $F(1, 28) = 6.114, P < 0.05$; Group: $F(1, 28) = 9.662, P < 0.01$; Interaction: $F(1, 28) = 2.828, P = 0.1$]; spinal cord [TPPU: $F(1, 28) = 6.981, P < 0.05$; Group: $F(1, 28) = 3.933, P = 0.06$; Interaction: $F(1, 28) = 7.76, P < 0.01$]; liver [TPPU: $F(1, 28) = 0.7191, P = 0.4$; Group: $F(1, 28) = 0.015, P = 0.9$; Interaction: $F(1, 28) = 0.6986, P = 0.41$]; kidney [TPPU: $F(1, 28) = 6.278, P < 0.05$; Group: $F(1, 28) = 14.19, P < 0.001$; Interaction: $F(1, 28) = 6.607, P < 0.05$]; gut [TPPU: $F(1, 28) = 0.3, P = 0.86$; Group: $F(1, 28) = 0.3095, P = 0.58$; Interaction: $F(1, 28) = 0.9039, P = 0.34$]. Data are reported as the mean \pm SEM ($n = 8$). $^{*}P < 0.05$, $^{**}P < 0.01$, $^{***}P < 0.001$. AHR aryl hydrocarbon receptor, CYP1A1 cytochrome P450, family 1, subfamily A, polypeptide 1, CYP1B1 cytochrome P450, family 1, subfamily B, polypeptide 1, sEH soluble epoxide hydrolase, mPFC medial prefrontal cortex, NS not significant, SNI spared nerve injury, Sus susceptible, TPPU 1-trifluoromethoxyphenyl-3-(1-propionyl piperidin-4-yl) urea, TSPO translocator protein, Veh vehicle

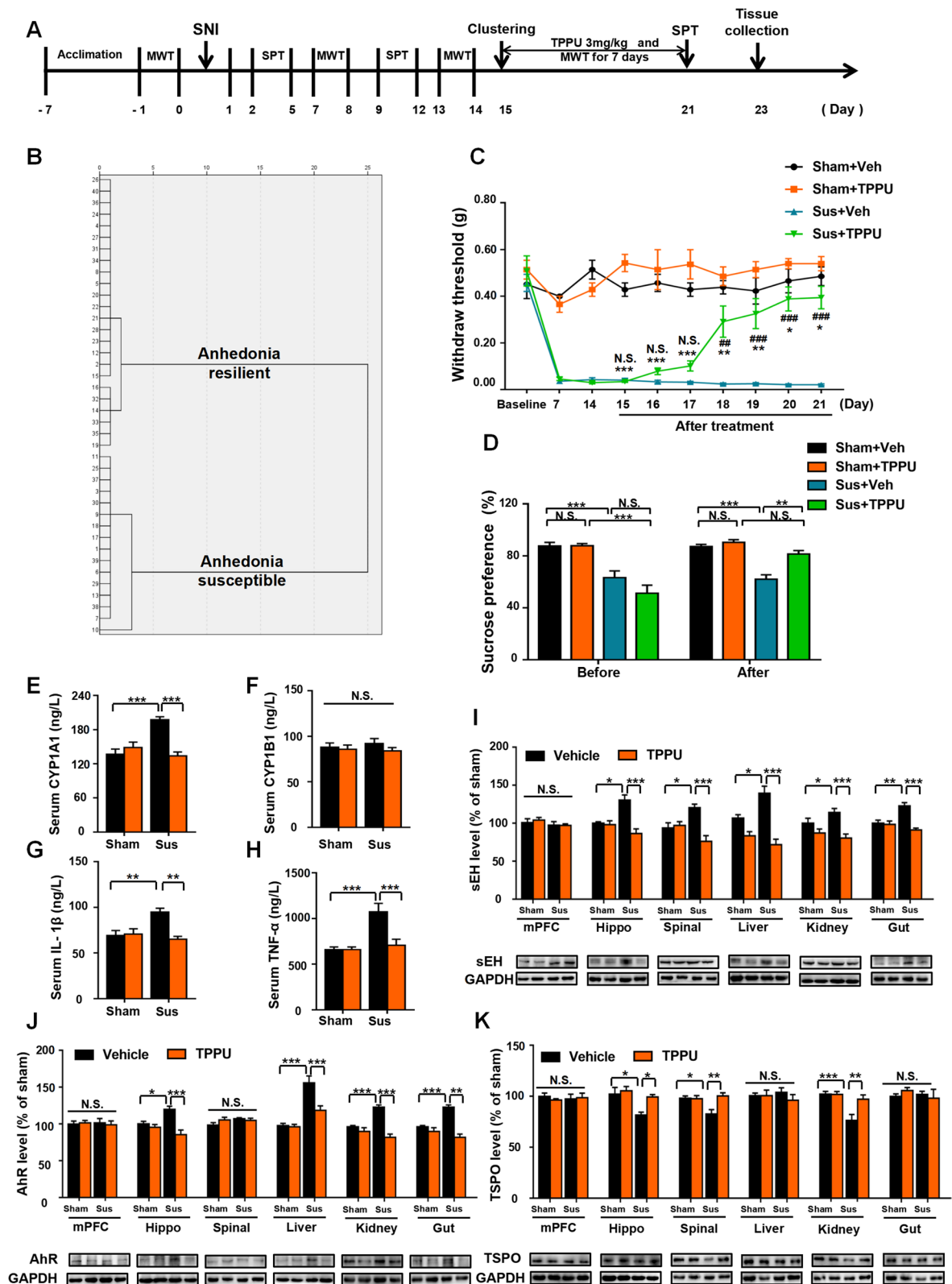


Fig. 3 (See legend on previous page.)

Discussion

Despite suffering from similar nociceptive damage, only some of the SNI mice exhibited the anhedonia phenotype. The tissue levels of sEH were increased in the mPFC, hippocampus, spinal cord, liver, kidney, and gut, but not in the ACC, NAc, striatum, cerebellum, heart, muscle, and vessels in anhedonia-susceptible mice compared with sham or anhedonia-resilient mice. We also found that the sEH level in selected tissues was negatively correlated with MWT scores, whereas the scores of the SPT positively correlated with the scores of the MWT. This suggests that sEH levels are closely related to neuropathic pain and that the results of the behavioral tests also changed after the onset of pain. Furthermore, TPPU not only reduced sEH protein levels, but also improved the anhedonia and hyperalgesia behaviors. In addition, we found that TPPU reduced the serum levels of inflammatory cytokines and CYP1A1. More importantly, the levels of two other proteins, AHR and TSPO, were also altered in selected tissues. Surprisingly, pretreatment with an AHR agonist attenuated the antidepressant-like but not the analgesic effect of TPPU. Furthermore, a TSPO agonist exerted a TPPU-like antidepressant effect.

Both chronic pain and depression seriously affect the patients' quality of life affected by them [48, 49]. However, they are frequently encountered clinically, thus increasing the morbidity and recurrence rates and rendering treatment more difficult [50]. According to epidemiological studies, chronic pain in patients treated for depression is as high as 51.8–59.1%; moreover, depression in patients with chronic pain reportedly ranges from 18 to 85% [51–54]. In preclinical studies, persistent pain

frequently induced depression-like behaviors [55]. Furthermore, chronic inflammatory pain and neuropathic pain often lead to hyperalgesia in animals. Some animals simultaneously exhibit anhedonia and behavioral despair [41, 56]. In this study, a hierarchical cluster analysis classified SNI mice into two clusters: one group (approximately 44%, anhedonia-like symptoms) had decreased scores in the SPT, whereas the other group (approximately 56%, without anhedonia-like symptoms) exhibited sucrose preference, similar to that observed in sham-operated mice and consistent with our previous report [57].

We found increased levels of sEH in the mPFC, hippocampus, spinal cord, liver, kidney, and gut. The liver, kidney, and intestine are important organs involved in immune response and the release of inflammatory cytokines. The mPFC, hippocampus, and spinal cord play an integral role in the pathogenesis of depression and pain [41, 58–61]. Recent preclinical studies showed that the expression levels of sEH in the mPFC, striatum, and hippocampus were higher in mice with depression-like behaviors than they were in control mice. Moreover, *sEH*-KO mice showed resilience to repeated social defeat stress [21]. In addition, sEH inhibitors also significantly relieved hyperalgesia in rats with chronic pain [62]. Accordingly, in the present study, we found that TPPU inhibited the expression of sEH and decreased the release of inflammatory cytokines, thus exerting analgesic and antidepressant effects.

AHR controls the conversion of PUFAs to EETs by regulating the transcription of the *CYP* family of genes [63]. It was interesting to detect an increased serum

(See figure on next page.)

Fig. 4 An AHR agonist attenuated the antidepressant effects, but not the analgesic effects of TPPU. **A** Schedule of the experiment. SNI surgery was performed after acclimation. CH-223191 (10 mg/kg, once daily) and TPPU (3 mg/kg, once daily) were administered orally for 7 consecutive days, starting at 14 after SNI. FICZ (100 µg/mg) was administered orally on day 14. MWT was measured on days 7, 14, 15, 16, 17, 18, 19, 20, and 21 after SNI. The SPT was performed on days 5, 12, and 21 after SNI. **B** Dendrogram of the hierarchical clustering analysis. A total of 33 SNI mice were classified into anhedonia-susceptible and anhedonia-resilient groups based on SPT scores. **C** MWT [Time: $F(9, 45) = 61.2, P < 0.001$; Group: $F(4, 20) = 128.8, P < 0.001$; Interaction: $F(36, 180) = 8.887, P < 0.001$] was measured on days 7, 14, 15, 16, 17, 18, 19, 20, and 21 after SNI in the Sham, Sus, Sus + CH-223191, Sus + FICZ, and Sus + FICZ + TPPU groups. *** $P < 0.001$, Sus group vs. Sus + FICZ + TPPU group; ### $P < 0.001$, Sus + FICZ group vs. Sus + FICZ + TPPU group. **D** The SPT [$F(4, 25) = 10.86, P < 0.001$] was performed in the sham, Sus, Sus + CH-223191, Sus + FICZ, and Sus + FICZ + TPPU groups on day 21 after SNI. * $P < 0.05$, ** $P < 0.01$. **E** CYP1A1 level in the serum [$F(4, 25) = 6.211, P < 0.01$]. **F** CYP1B1 level in the serum [$F(4, 25) = 1.964, P = 0.13$]. **G** IL-1 β level in the serum [$F(4, 25) = 15.85, P < 0.01$]. **H** TNF- α level in the serum [$F(4, 25) = 4.449, P < 0.01$]. **I** Effects of TPPU on sEH expression. mPFC [$F(4, 25) = 8.255, P < 0.001$]; hippocampus [$F(4, 25) = 21.93, P < 0.001$]; spinal cord [$F(4, 25) = 7.137, P < 0.001$]; liver [$F(4, 25) = 3.81, P < 0.05$]; kidney [$F(4, 25) = 7.236, P < 0.001$]; gut [$F(4, 25) = 12.33, P < 0.001$]. * $P < 0.05$, ** $P < 0.01$, *** $P < 0.001$. **J** Effects of TPPU on AHR expression. mPFC [$F(4, 25) = 5.272, P < 0.01$]; hippocampus [$F(4, 25) = 48.4, P < 0.001$]; spinal cord [$F(4, 25) = 0.2683, P = 0.90$]; liver [$F(4, 25) = 18.69, P < 0.001$]; kidney [$F(4, 25) = 41.8, P < 0.001$]; gut [$F(4, 25) = 5.395, P < 0.01$]. * $P < 0.05$, ** $P < 0.01$, *** $P < 0.001$. **K** Effects of TPPU on TSPO expression. mPFC [$F(4, 25) = 0.9551, P = 0.45$]; hippocampus [$F(4, 25) = 8.753, P < 0.001$]; spinal cord [$F(4, 25) = 6.161, P < 0.01$]; liver [$F(4, 25) = 0.3481, P = 0.84$]; kidney [$F(4, 25) = 2.627, P = 0.059$]; gut [$F(4, 25) = 0.9321, P = 0.46$]. * $P < 0.05$, ** $P < 0.01$, *** $P < 0.001$. AHR aryl hydrocarbon receptor, CYP1A1 cytochrome P450, family 1, subfamily A, polypeptide 1, CYP1B1 cytochrome P450, family 1, subfamily B, polypeptide 1, FICZ 6-formylindolo[3,2-b]carbazole, sEH soluble epoxide hydrolase, mPFC medial prefrontal cortex, NS not significant, SNI spared nerve injury, Sus susceptible, TPPU 1-trifluoromethoxyphenyl-3-(1-propionyl)piperidin-4-yl) urea, TSPO translocator protein

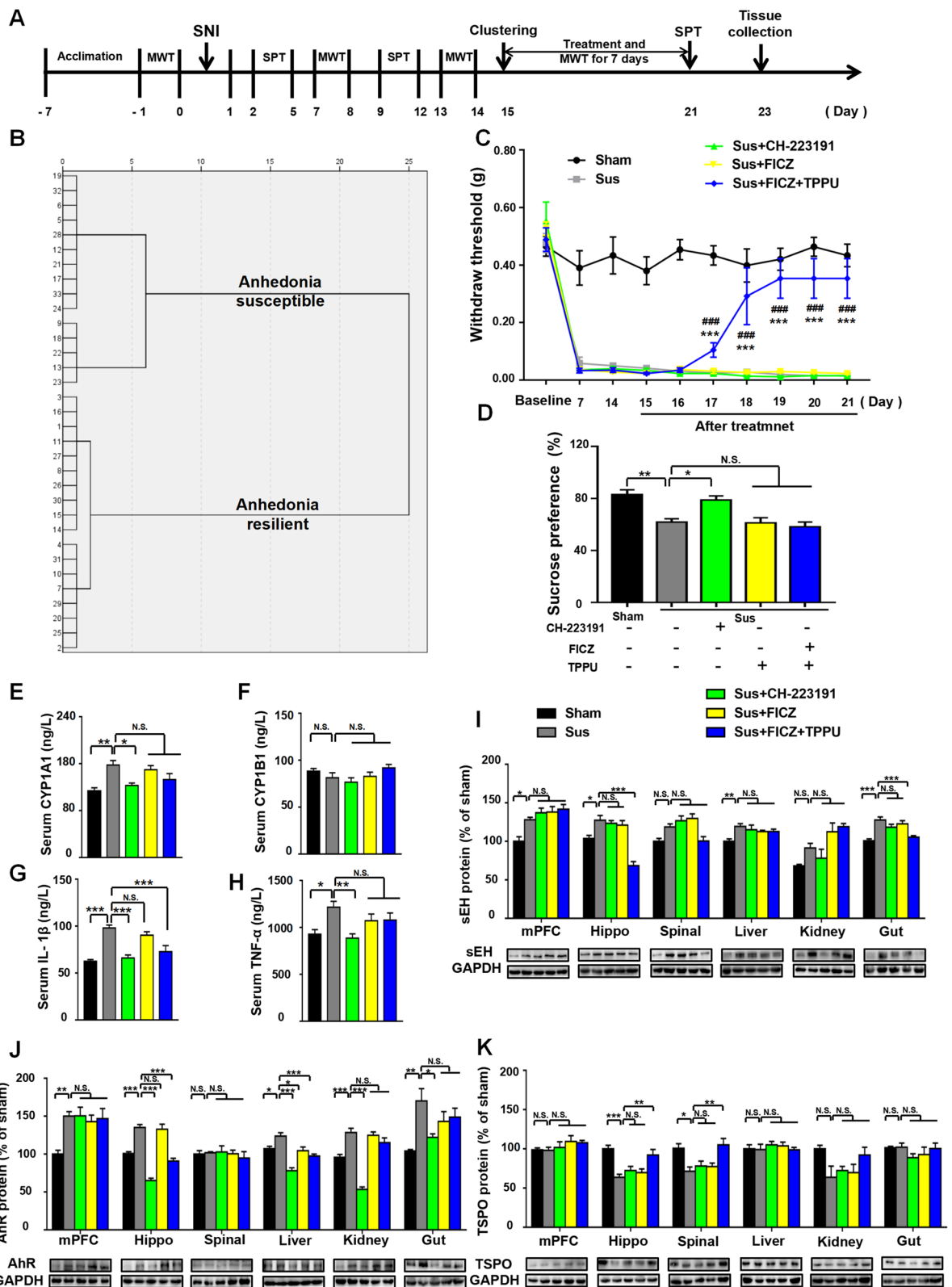


Fig. 4 (See legend on previous page.)

Table 1 Stimulation/inhibition of AHR receptor (AHR)-responsive luciferase reporter gene activity in H1L6.1c3 cells by sample extracts

Chemical treatment	Agonist activity	Antagonist activity
TCDD	100 ± 29.14	100 ± 28.68
TPPU	− 0.70 ± 2.66	85.18 ± 31.23

Results are expressed as the mean ± SD of triplicate incubations of each sample and an asterisk (*) indicates those values significantly greater than the background activity in the DMSO blank at $P < 0.05$ as determined by the Students t-test. Results in this table demonstrate that no chemical significantly induced AHR-dependent reporter gene activity above background activity or antagonized induction by the reference standard, TCDD. (Table 1)

level of CYP1A1, but not CYP1B1 in anhedonia-susceptible mice. This discrepancy may result from the different spectra of eicosanoids obtained from ARA in the CYP family. CYP1A1 tends to produce HETEs, whereas CYP1B1 favors EETs [64]. Together with anti-inflammatory EETs, PUFAs are also involved in the biosynthesis of pro-inflammatory mediators through COX and LOX pathways and CYP hydroxylation [65]. Thus, sEH amplified the inflammatory reaction by deactivating EETs and other EpEAs. Several studies suggested AHR overactivation in the hippocampus contributes to neuroinflammatory diseases [25]. Similarly, we found significantly elevated AHR expression in the hippocampus of anhedonia-susceptible mice, which was consistent with changes in sEH. However, there were no changes in the spinal cord. Moreover, TPPU failed to exert an antidepressant-like effect after pretreatment with an AHR agonist. This suggests that AHR signaling is involved exclusively in the occurrence of depression-like symptoms and explains why AHR expression in the spinal cord was not different between the anhedonia-susceptible mice and the sham group.

In addition to synergistically promoting depressive symptoms with AHR, sEH can also inhibit normal TSPO function by inducing the co-occurrence of pain and

depression. EETs promoted the transport of cholesterol in mitochondria via TSPO, leading to the production of neurosteroids [66]. In turn, neurosteroids can affect neuron survival and differentiation by regulating neurotrophic factors and anti-inflammatory cytokines [67, 68]. The activation of TSPO in the spinal cord relieves neuropathic and inflammatory pain [69]. It has been reported that steroidogenic acute regulatory protein (StARD1) and TSPO cooperatively exert antihyperalgesic effect by EETs or sEHs [70]. Furthermore, TSPO overexpression in the hippocampus attenuated depression-like behaviors associated with increased neurosteroid synthesis [71]. In the present study, we found decreased expression of TSPO in the hippocampus and spinal cord in anhedonia-susceptible mice, which might stem from the increased activity of sEH. More importantly, the analgesic and antidepressant effects of the TSPO agonist did not reduce the peripheral levels of inflammatory cytokines, which suggests that the primary therapeutic target of TSPO in the brain. Previous studies showed that the low concentration of neurosteroids produced by the neuronal autocrine system quickly and efficiently exerted pharmacological effects locally [72, 73]. We need further devote our effort to explore the other potential agents for chronic pain and depression comorbidity.

Conclusions

Our present study results suggest that elevated levels of sEH play an important role in neuropathic pain with anhedonia (Fig. 6). Moreover, TPPU may alleviate the anhedonia and pain behaviors in two ways: (1) reducing the release of peripheral inflammatory factors via the inhibition of AHR signaling, to function as an antidepressant; and (2) improving depressive-like and hyperalgesic behaviors by promoting the synthesis of neurosteroids involved in TSPO signaling. Therefore, these findings provide novel therapeutic targets for chronic pain and depression comorbidity.

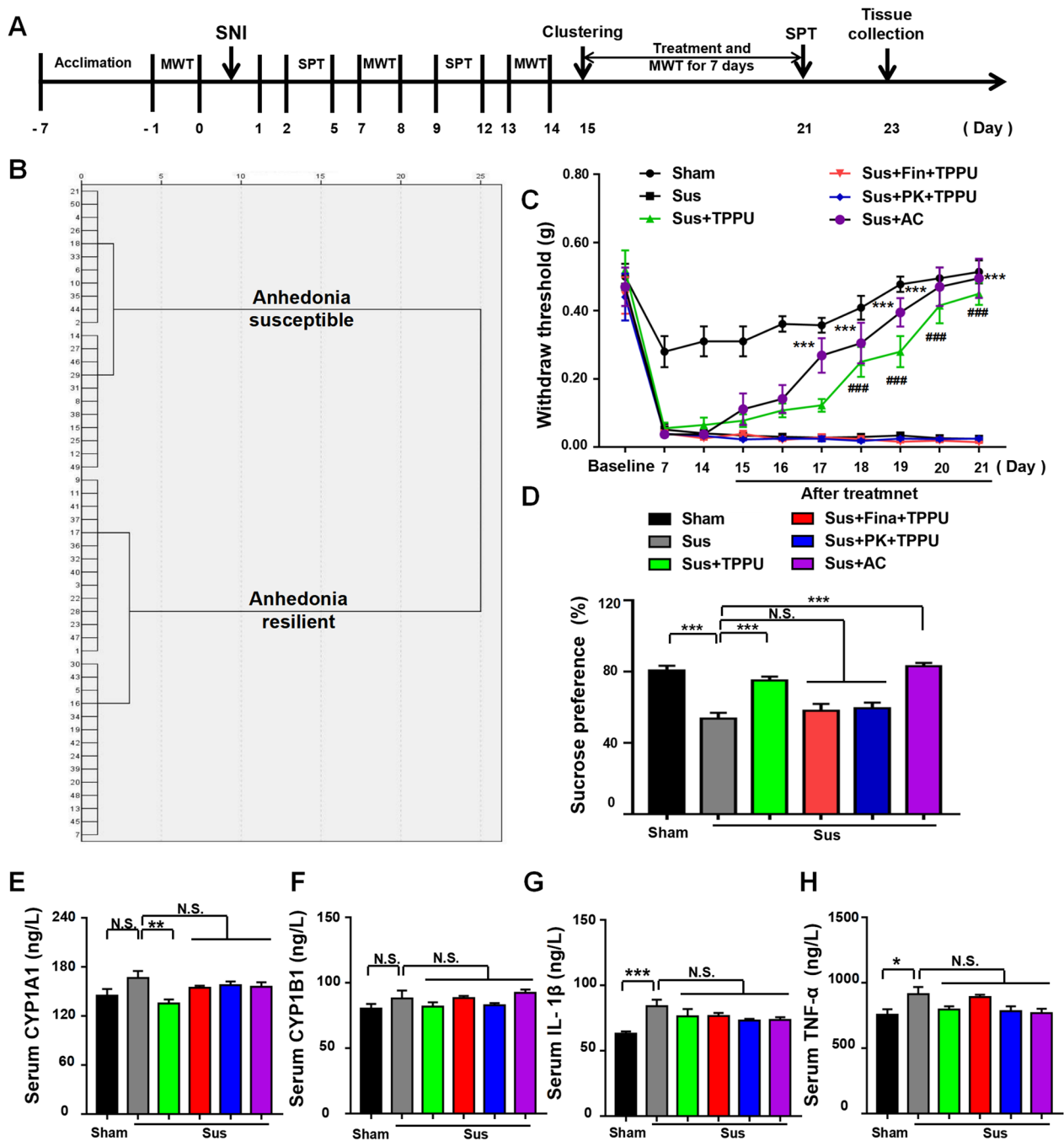


Fig. 5 A TSPO antagonist attenuated the antidepressant and analgesic effects of TPPU. **A** Schedule of the experiment. SNI surgery was performed on day 0 after acclimation. Finasteride (10 mg/kg, once daily) or PK-11195 (3 mg/kg, once daily) was administered orally together with TPPU (3 mg/kg, once daily) for 7 consecutive days, starting at day 14 after SNI. AC-5216 (5 mg/mg) was administered orally from day 14 to day 21. MWT was measured on days 7, 14, 15, 16, 17, 18, 19, 20, and 21 after SNI. The SPT was performed on days 5, 12, and 21 after SNI. **B** Dendrogram of the hierarchical clustering analysis. A total of 36 SNI mice were classified into anhedonia-susceptible and anhedonia-resilient groups based on SPT scores. **C** MWT [Time: $F(9, 63) = 73.44, P < 0.001$; Group: $F(5, 35) = 156.5, P < 0.001$; Interaction: $F(45, 315) = 9.604, P < 0.001$] was measured on days 7, 14, 15, 16, 17, 18, 19, 20, and 21 after SNI in the Sham, Sus, Sus + TPPU, Sus + Fina + TPPU, Sus + PK + TPPU, and Sus + AC groups. $***P < 0.001$, Sus group vs. Sus + AC group; $###P < 0.001$, Sus group vs. Sus + TPPU group. **D** The SPT [$F(5, 42) = 18.98, P < 0.001$] was performed on day 21 after SNI in the Sham, Sus, Sus + TPPU, Sus + Fina + TPPU, Sus + PK + TPPU, and Sus + AC groups. $***P < 0.001$. **E** CYP1A1 level in the serum [$F(5, 42) = 3.299, P < 0.05$]. **F** CYP1B1 level in the serum [$F(5, 42) = 1.825, P = 0.13$]. **G** IL-1β level in the serum [$F(5, 42) = 4.101; P < 0.01$]. **H** TNF-α level in the serum [$F(5, 42) = 3.41; P < 0.05$]. $*P < 0.05$, $**P < 0.01$, $***P < 0.001$. AC AC-5216, AHR aryl hydrocarbon receptor, CYP1A1 cytochrome P450, family 1, subfamily A, polypeptide 1, CYP1B1 cytochrome P450, family 1, subfamily B, polypeptide 1; Fina, finasteride, NS not significant, SNI spared nerve injury; Sus, susceptible, TPPU 1-trifluoromethoxyphenyl-3-(1-propionylpiperidin-4-yl) urea, PK PK-11195

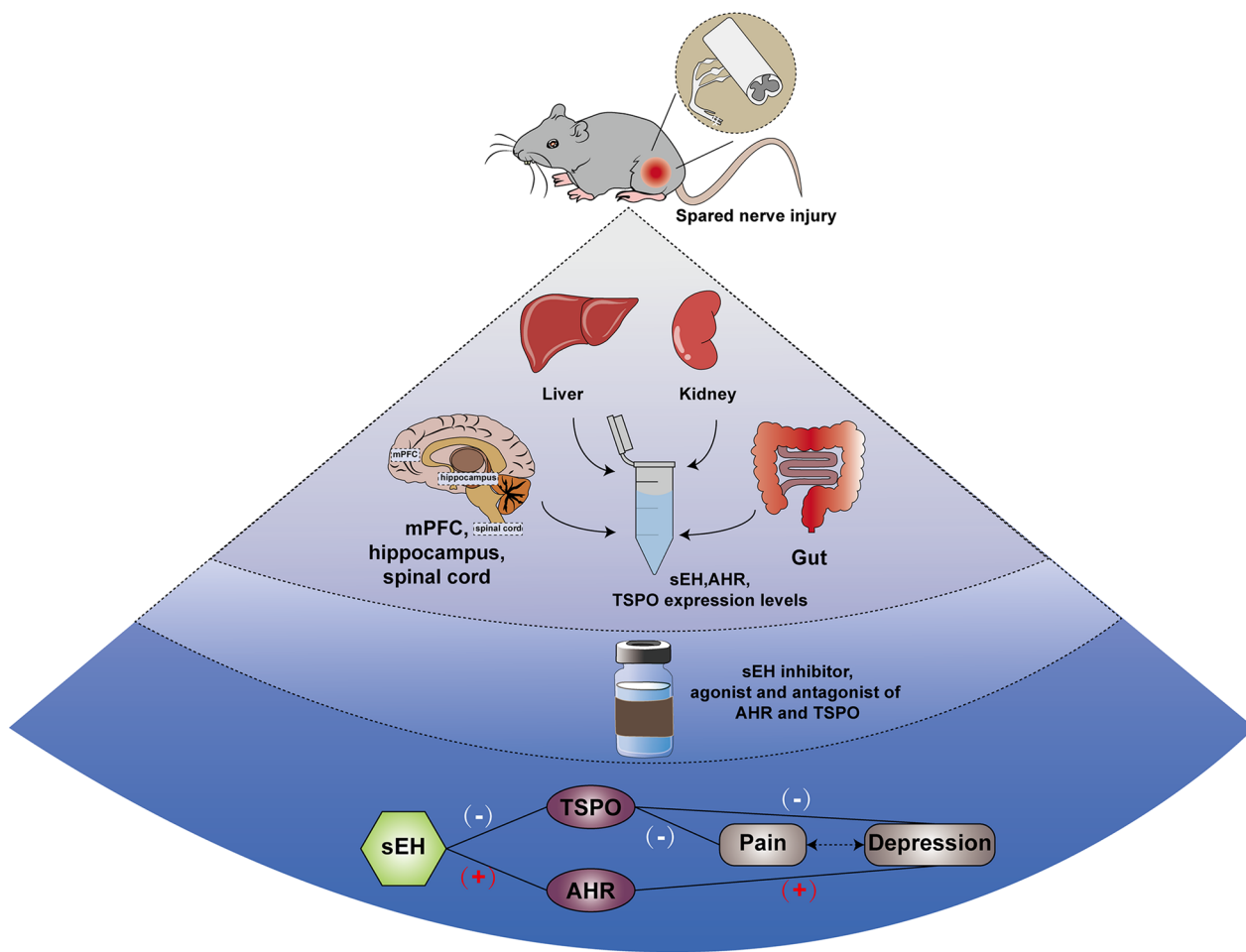


Fig. 6 The soluble epoxide hydrolase inhibitor TPPU improves comorbidity of chronic pain and depression via AHR and TSPO signaling. Spared nerve injury (SNI) was used for the rodent model of pain-depression comorbidity. sEH inhibitor exerted antidepressant-like and analgesic effects in two ways: (1) inhibiting AHR signaling to function as antidepressant; and (2) improving depressive-like and hyperalgesic behaviors by increasing the TSPO protein levels

Abbreviations

sEH	Soluble epoxide hydrolase
SPT	Sucrose preference test
SNI	Spared nerve injury
mPFC	Medial prefrontal cortex
IL-1β	Interleukin 1β
TNF-α	Tumor necrosis factor α
MWT	Mechanical withdrawal threshold
AHR	Aryl hydrocarbon receptor
TSPO	Translocator protein
ARA	Arachidonic acid
CYP450s	Cytochrome P450s
EpFAs	Epoxy fatty acids
EETs	Epoxyeicosatrienoic acids
PUFAs	Polyunsaturated fatty acids
EPA	Eicosapentaenoic acid
DHA	Docosahexaenoic acid
EEQs	Epoxyeicosatetraenoic acids
EDPs	Epoxydocosapentaenoic acids
EpFAs	Epoxy-fatty acids
VCAM-1	Vascular cell adhesion molecule 1
ICAM-1	Intercellular adhesion molecule 1
E-selectin	Endothelial cell-selective adhesion molecule

NF-κB	Nuclear factor κB
DHETs	Dihydroxyeicosatrienoic acids
sEHIs	sEH inhibitors
LPS	Lipopolysaccharide
ARNT	AHR nuclear translocator
HETEs	Hydroxyeicosatetraenoic acids

Supplementary Information

The online version contains supplementary material available at <https://doi.org/10.1186/s12967-023-03917-x>.

Additional file 1: Figure S1. Dendrogram of the hierarchical clustering analysis. A total of 27 SNI mice were classified into anhedonia-susceptible and anhedonia-resilient groups by a hierarchical cluster analysis of the SPT results. SNI, spared nerve injury; SPT, sucrose preference test. **Figure S2.** Dendrogram of the hierarchical clustering analysis. A total of 52 SNI mice were classified into anhedonia-susceptible and anhedonia-resilient groups by a hierarchical cluster analysis of the SPT results. SNI, spared nerve injury; SPT, sucrose preference test. **Table S1.** (Additional material for figure 1B). **Table S2.** (Additional material for figure 3B). **Table S3.** (Additional material for figure 4B). **Table S4.** (Additional material for figure S1). **Table S5.** (Additional material for figure 5B). **Table S6.** (Additional material for S2).

Acknowledgements

We would like to appreciate all of the researchers for their efforts, time and contributions.

Author contributions

LA, WZ and LS conceived the idea of the research and wrote the manuscript. CBM, WD, LH and HC acquired all data. HT, ZX and WY performed data analyses. LC, BDH, KH and CY reviewed the manuscript. All authors read and approved the final manuscript.

Funding

This study was supported by grants from the National Natural Science Foundation of China (to C.Y., 82271254, 81974171 and 81703482; to D.W., 82201420; To C.H., 82101270), National Key R & D Program of China (to A.L., No. 2020YFC2009002), Innovative and Entrepreneurial Team of Jiangsu Province (to C.Y., JSSCTD202144), Natural Science Foundation of Jiangsu Province grant (to C.L., BK20211382; to C.H., BK20210975), Japan Society for the Promotion of Science, Japan (to K.H., 21H00184, 21H05612, and 21H02846), the National Institute of Environmental Health Sciences of the National Institutes of Health under RIVER Award R35ES030443 (B.D.H.), and the National Institute of Environmental Health Sciences of the National Institutes of Health under Superfund Program P42ES004699 (B.D.H.).

Availability of data and materials

The datasets used during this study are available from the corresponding author on reasonable request.

Declarations

Ethics approval and consent to participate

Two month-old male C57BL/6 mice (body weight 20–25 g) were purchased from the Animal Center of Tongji Hospital in this study. The study was conducted according to the recommendations in the Guide for the Care and Use of Laboratory Animals and under protocols approved by the Experimental Animal Committee of Tongji Hospital, Tongji Medical College, Huazhong University of Science and Technology (Wuhan, China).

Consent for publication

All the authors give consent.

Competing interests

EicOsis Human Health is a private company co-founded by BDH and has licensed several patents from the University of California on sEH and is in human clinical trials on sEH.

Received: 26 September 2022 Accepted: 23 January 2023

Published online: 02 February 2023

References

1. Fillingim RB. Individual differences in pain: understanding the mosaic that makes pain personal. *Pain*. 2017;158(Suppl 1):11–8.
2. Yang C, et al. AMPA receptor activation-independent antidepressant actions of ketamine metabolite (S)-norketamine. *Biol Psychiatry*. 2018;84(8):591–600.
3. Yin N, et al. The role of microglia in chronic pain and depression: innocent bystander or culprit? *Psychopharmacology*. 2021;238(4):949–58.
4. Mazereeuw G, Sullivan MD, Juurlink DN. Depression in chronic pain: might opioids be responsible? *Pain*. 2018;159(11):2142–5.
5. Beurel E, Toups M, Nemeroff CB. The bidirectional relationship of depression and inflammation: double trouble. *Neuron*. 2020;107(2):234–56.
6. Ji RR, Chamesian A, Zhang YQ. Pain regulation by non-neuronal cells and inflammation. *Science*. 2016;354(6312):572–7.
7. Ji RR, et al. Neuroinflammation and central sensitization in chronic and widespread pain. *Anesthesiology*. 2018;129(2):343–66.
8. Matsuda M, Huh Y, Ji RR. Roles of inflammation, neurogenic inflammation, and neuroinflammation in pain. *J Anesth*. 2019;33(1):131–9.
9. Dean B, et al. Regionally-specific changes in levels of tumour necrosis factor in the dorsolateral prefrontal cortex obtained postmortem from subjects with major depressive disorder. *J Affect Disord*. 2010;120(1–3):245–8.
10. Spector AA, et al. Epoxyeicosatrienoic acids (EETs): metabolism and biochemical function. *Prog Lipid Res*. 2004;43(1):55–90.
11. Zhang G, Kodani S, Hammock BD. Stabilized epoxygenated fatty acids regulate inflammation, pain, angiogenesis and cancer. *Prog Lipid Res*. 2014;53:108–23.
12. Node K, et al. Anti-inflammatory properties of cytochrome P450 epoxygenase-derived eicosanoids. *Science*. 1999;285(5431):1276–9.
13. Zhao G, et al. Delivery of AAV2-CYP2J2 protects remnant kidney in the 5/6-nephrectomized rat via inhibition of apoptosis and fibrosis. *Hum Gene Ther*. 2012;23(7):688–99.
14. Bystrom J, et al. Endogenous epoxygenases are modulators of monocyte/macrophage activity. *PLoS ONE*. 2011;6(10): e26591.
15. Huang H, Weng J, Wang MH. EETs/sEH in diabetes and obesity-induced cardiovascular diseases. *Prostaglandins Other Lipid Mediat*. 2016;125:80–9.
16. Marowsky A, et al. Distribution of soluble and microsomal epoxide hydrolase in the mouse brain and its contribution to cerebral epoxyeicosatrienoic acid metabolism. *Neuroscience*. 2009;163(2):646–61.
17. Wagner K, et al. Soluble epoxide hydrolase inhibition is antinociceptive in a mouse model of diabetic neuropathy. *J Pain*. 2014;15(9):907–14.
18. Rose TE, et al. 1-Aryl-3-(1-acylpiperidin-4-yl)urea inhibitors of human and murine soluble epoxide hydrolase: structure-activity relationships, pharmacokinetics, and reduction of inflammatory pain. *J Med Chem*. 2010;53(19):7067–75.
19. Hashimoto K. Soluble epoxide hydrolase: a new therapeutic target for depression. *Expert Opin Ther Targets*. 2016;20(10):1149–51.
20. Wu J, et al. Inhibition of soluble epoxide hydrolase (sEH) protects hippocampal neurons and reduces cognitive decline in type 2 diabetic mice. *Eur J Neurosci*. 2021;53(8):2532–40.
21. Ren Q, et al. Gene deficiency and pharmacological inhibition of soluble epoxide hydrolase confers resilience to repeated social defeat stress. *Proc Natl Acad Sci USA*. 2016;113(13):E1944–52.
22. Gautheron J, Jéru I. The multifaceted role of epoxide hydrolases in human health and disease. *Int J Mol Sci*. 2020. <https://doi.org/10.3390/ijms2010013>.
23. Kyoreva M, et al. CYP1A1 enzymatic activity influences skin inflammation via regulation of the AHR pathway. *J Invest Dermatol*. 2021;141(6):1553–1563.e3.
24. Vogel CFA, et al. The aryl hydrocarbon receptor as a target of environmental stressors - Implications for pollution mediated stress and inflammatory responses. *Redox Biol*. 2020;34: 101530.
25. Ramos-García NA, et al. Aryl hydrocarbon receptor in post-mortem hippocampus and in serum from young, elder, and Alzheimer's patients. *Int J Mol Sci*. 2020. <https://doi.org/10.3390/ijms21061983>.
26. Imig JD, Hammock BD. Soluble epoxide hydrolase as a therapeutic target for cardiovascular diseases. *Nat Rev Drug Discov*. 2009;8(10):794–805.
27. Morisseau C, Hammock BD. Impact of soluble epoxide hydrolase and epoxyeicosanoids on human health. *Annu Rev Pharmacol Toxicol*. 2013;53:37–58.
28. Neavin DR, et al. The role of the aryl hydrocarbon receptor (AHR) in immune and inflammatory diseases. *Int J Mol Sci*. 2018. <https://doi.org/10.3390/ijms19123851>.
29. Chen WC, et al. Aryl hydrocarbon receptor modulates stroke-induced astrogliosis and neurogenesis in the adult mouse brain. *J Neuroinflamm*. 2019;16(1):187.
30. Zhou D, Ji L, Chen Y. TSPO Modulates IL-4-Induced Microglia/Macrophage M2 Polarization via PPAR-γ Pathway. *J Mol Neurosci*. 2020;70(4):542–9.
31. Wolf L, et al. Enhancing neurosteroid synthesis—relationship to the pharmacology of translocator protein (18 kDa) (TSPO) ligands and benzodiazepines. *Pharmacopsychiatry*. 2015;48(2):72–7.
32. Xiong B, et al. Identification of Koumine as a translocator protein 18 kDa positive allosteric modulator for the treatment of inflammatory and neuropathic pain. *Front Pharmacol*. 2021;12: 692917.
33. Hernstadt H, et al. Spinal translocator protein (TSPO) modulates pain behavior in rats with CFA-induced monoarthritis. *Brain Res*. 2009;1286:42–52.

34. Roca-Agujetas V, et al. Cholesterol alters mitophagy by impairing optineurin recruitment and lysosomal clearance in Alzheimer's disease. *Mol Neurodegener.* 2021;16(1):15.
35. Navia-Pelaez JM, et al. Normalization of cholesterol metabolism in spinal microglia alleviates neuropathic pain. *J Exp Med.* 2021. <https://doi.org/10.1084/jem.20202059>.
36. Wang DS, et al. Anxiolytic-like effects of translocator protein (TSPO) ligand ZBD-2 in an animal model of chronic pain. *Mol Pain.* 2015;11:16.
37. Shen L, et al. A potent soluble epoxide hydrolase inhibitor, t-AUCB, modulates cholesterol balance and oxidized low density lipoprotein metabolism in adipocytes in vitro. *Biol Chem.* 2014;395(4):443–51.
38. Domingues MF, et al. Soluble epoxide hydrolase and brain cholesterol metabolism. *Front Mol Neurosci.* 2019;12:325.
39. Norman GJ, et al. Stress and IL-1beta contribute to the development of depressive-like behavior following peripheral nerve injury. *Mol Psychiatry.* 2010;15(4):404–14.
40. Bourquin AF, et al. Assessment and analysis of mechanical allodynia-like behavior induced by spared nerve injury (SNI) in the mouse. *Pain.* 2006;122(1–2):14.e1–14.
41. Li S, et al. Role of Keap1-Nrf2 signaling in anhedonia symptoms in a rat model of chronic neuropathic pain: improvement with sulforaphane. *Front Pharmacol.* 2018;9:887.
42. Mohammadi-Bardbori A, Omidi M, Arabnezhad MR. Impact of CH223191-induced mitochondrial dysfunction on its aryl hydrocarbon receptor agonistic and antagonistic activities. *Chem Res Toxicol.* 2019;32(4):691–7.
43. Zang X, et al. Regulation of proinflammatory monocyte activation by the kynurenine-AhR axis underlies immunometabolic control of depressive behavior in mice. *Faseb j.* 2018;32(4):1944–56.
44. Li L, et al. Overexpression of the 18 kDa translocator protein (TSPO) in the hippocampal dentate gyrus produced anxiolytic and antidepressant-like behavioural effects. *Neuropharmacology.* 2017;125:117–28.
45. Kita A, et al. Antianxiety and antidepressant-like effects of AC-5216, a novel mitochondrial benzodiazepine receptor ligand. *Br J Pharmacol.* 2004;142(7):1059–72.
46. He G, et al. Cell-Based Assays for Identification of Aryl Hydrocarbon Receptor (AhR) Activators, in Optimization in Drug Discovery. In: Caldwell GW, Yan Z, editors, et al. *Vitro Methods.* Totowa, NJ: Humana Press; 2014. p. 221–35.
47. Bu J, et al. Comparative study of hydrochemical classification based on different hierarchical cluster analysis methods. *Int J Environ Res Public Health.* 2020. <https://doi.org/10.3390/ijerph17249515>.
48. Kohrt BA, Griffith JL, Patel V. Chronic pain and mental health: integrated solutions for global problems. *Pain.* 2018;159(Suppl 1):85–90.
49. Schramm E, et al. Review of dysthymia and persistent depressive disorder: history, correlates, and clinical implications. *Lancet Psychiatry.* 2020;7(9):801–12.
50. Zhou W, et al. A neural circuit for comorbid depressive symptoms in chronic pain. *Nat Neurosci.* 2019;22(10):1649–58.
51. Lee P, et al. Frequency of painful physical symptoms with major depressive disorder in asia: relationship with disease severity and quality of life. *J Clin Psychiatry.* 2009;70(1):83–91.
52. Agüera-Ortiz L, et al. Pain as a symptom of depression: prevalence and clinical correlates in patients attending psychiatric clinics. *J Affect Disord.* 2011;130(1–2):106–12.
53. Bair MJ, et al. Depression and pain comorbidity: a literature review. *Arch Intern Med.* 2003;163(20):2433–45.
54. Williams LS, et al. Prevalence and impact of depression and pain in neurology outpatients. *J Neurol Neurosurg Psychiatry.* 2003;74(11):1587–9.
55. Campbell LC, Clauw DJ, Keefe FJ. Persistent pain and depression: a biopsychosocial perspective. *Biol Psychiatry.* 2003;54(3):399–409.
56. Le AM, et al. AMPAkinases have novel analgesic properties in rat models of persistent neuropathic and inflammatory pain. *Anesthesiology.* 2014;121(5):1080–90.
57. Fang X, et al. Brain-derived neurotrophic factor-TrkB signaling in the medial prefrontal cortex plays a role in the anhedonia-like phenotype after spared nerve injury. *Eur Arch Psychiatry Clin Neurosci.* 2020;270(2):195–205.
58. Zheng M, Tian Z. Liver-mediated adaptive immune tolerance. *Front Immunol.* 2019;10:2525.
59. Rucker AJ, Rudemiller NP, Crowley SD. Salt, hypertension, and immunity. *Annu Rev Physiol.* 2018;80:283–307.
60. Yeoh YK, et al. Gut microbiota composition reflects disease severity and dysfunctional immune responses in patients with COVID-19. *Gut.* 2021;70(4):698–706.
61. Zhang R, et al. Mechanisms of acupuncture-electroacupuncture on persistent pain. *Anesthesiology.* 2014;120(2):482–503.
62. Wagner K, et al. Epoxy fatty acids mediate analgesia in murine diabetic neuropathy. *Eur J Pain.* 2017;21(3):456–65.
63. Yamaguchi M, Hankinson O. An aryl hydrocarbon receptor agonist suppresses the growth of human umbilical vein endothelial cells in vitro: potent effect with polyunsaturated fatty acids. *Int J Exp Pathol.* 2020;101(6):248–63.
64. Hankinson O. The role of AHR-inducible cytochrome P450s in metabolism of polyunsaturated fatty acids. *Drug Metab Rev.* 2016;48(3):342–50.
65. Sarparast M, et al. Cytochrome P450 metabolism of polyunsaturated fatty acids and neurodegeneration. *Nutrients.* 2020. <https://doi.org/10.3390/nu12113523>.
66. Wan L, et al. Epoxyeicosatrienoic acids: Emerging therapeutic agents for central post-stroke pain. *Pharmacol Res.* 2020;159: 104923.
67. Yilmaz C, et al. Neurosteroids as regulators of neuroinflammation. *Front Neuroendocrinol.* 2019;55: 100788.
68. Schaeffer V, et al. Sciatic nerve injury induces apoptosis of dorsal root ganglion satellite glial cells and selectively modifies neurosteroidogenesis in sensory neurons. *Glia.* 2010;58(2):169–80.
69. Wei XH, et al. The upregulation of translocator protein (18 kDa) promotes recovery from neuropathic pain in rats. *J Neurosci.* 2013;33(4):1540–51.
70. Inceoglu B, et al. Soluble epoxide hydrolase and epoxyeicosatrienoic acids modulate two distinct analgesic pathways. *Proc Natl Acad Sci USA.* 2008;105(48):18901–6.
71. Wang YL, et al. Microglial activation mediates chronic mild stress-induced depressive- and anxiety-like behavior in adult rats. *J Neuroinflammation.* 2018;15(1):21.
72. Schumacher M, et al. Neurosteroids in the Hippocampus: neuronal plasticity and memory. *Stress.* 1997;2(1):65–78.
73. Plassart-Schiess E, Baulieu EE. Neurosteroids: recent findings. *Brain Res Brain Res Rev.* 2001;37(1–3):133–40.

Publisher's Note

Springer Nature remains neutral with regard to jurisdictional claims in published maps and institutional affiliations.

Ready to submit your research? Choose BMC and benefit from:

- fast, convenient online submission
- thorough peer review by experienced researchers in your field
- rapid publication on acceptance
- support for research data, including large and complex data types
- gold Open Access which fosters wider collaboration and increased citations
- maximum visibility for your research: over 100M website views per year

At BMC, research is always in progress.

Learn more biomedcentral.com/submissions

